Sensing Distant Nuclear Spins with a Single Electron Spin

Shimon Kolkowitz, Quirin P. Unterreithmeier,* Steven D. Bennett, and Mikhail D. Lukin

Department of Physics, Harvard University, Cambridge, Massachusetts 02138, USA

(Received 23 April 2012; published 25 September 2012)

We experimentally demonstrate the use of a single electronic spin to measure the quantum dynamics of distant individual nuclear spins from within a surrounding spin bath. Our technique exploits coherent control of the electron spin, allowing us to isolate and monitor nuclear spins weakly coupled to the electron spin. Specifically, we detect the evolution of distant individual ^{13}C nuclear spins coupled to single nitrogen vacancy centers in a diamond lattice with hyperfine couplings down to a factor of 8 below the electronic spin bare dephasing rate. Potential applications to nanoscale magnetic resonance imaging and quantum information processing are discussed.

DOI: 10.1103/PhysRevLett.109.137601 PACS numbers: 76.60.Pc, 07.55.Ge, 71.55.−i, 76.30.Mi

Detection and control of the magnetic signals from nuclear spins is an important problem in science and technology. Single nuclear spin detection remains an outstanding goal in magnetic resonance imaging (MRI), with far-reaching implications from physics to medicine [1–3]. Likewise, nuclear spins stand out in quantum information science for their exceptional isolation from their environment, making them attractive qubit candidates. However, individual nuclear spins are extremely difficult to isolate and control. Utilizing the electronic spin associated with a single nitrogen-vacancy (NV) center in diamond to detect and control surrounding nuclei is a promising approach to this challenge. Early work has demonstrated that NV centers can be used to sense strongly coupled proximal nuclear spins [4–6]. This approach has been used to create a few-qubit quantum register [7,8], perform simple quantum algorithms [4,9], implement single shot readout of both nuclear and electronic spins [10,11], and demonstrate a multisecond quantum memory at room temperature [12].

In this Letter we show that the NV electronic spin can be used to isolate and probe the quantum dynamics of distant, weakly coupled individual carbon-13 nuclear spins. Our approach relies on dynamical decoupling sequences, which enhance the sensitivity to individual nuclear spins while suppressing NV electronic spin decoherence [13–19]. Crucially, this allows us to observe the coherent evolution of nuclear spins whose coupling to the NV is weaker than the limit imposed by the NV spin's inhomogenous dephasing rate, $1/T_2^*$. We demonstrate this capability by identifying single nuclear spins from amongst a bath of naturally abundant ^{13}C nuclear spins. The ability to isolate spins from within a bath is important for applications where surrounding nuclear spins cannot be avoided; moreover, it enables the use of these nuclear spins as a resource. In particular, our technique could be extended to harness weakly coupled nuclear spins in quantum registers [4,8–12], investigate the spatial extent of the NV electronic wave function [20–23], or detect individual spins outside of the diamond lattice for single spin MRI applications [1,2,13,24].

The central idea of this work is depicted in Fig. 1(c), and can be understood in terms of the coherent evolution of a single ^{13}C nuclear spin interacting with the NV electronic spin sensor. Through their interaction, the magnitude and orientation of the local magnetic field experienced by the ^{13}C spin depends on the NV spin state. Consequently, when the NV spin is prepared in a superposition of its energy eigenstates, the ^{13}C spin undergoes conditional Larmor precession around two different axes. During this precession the electron and nuclear spin become entangled and disentangled [5]. However, if the NV-nuclear coupling is weak then the two precession axes are similar and the resulting entanglement is small. The key idea of this work is to increase the degree of entanglement, and thus the measurable signal, by applying periodic π pulses, flipping the NV spin with a frequency matched to the precession of the ^{13}C spin. As shown schematically in Fig. 1(c), this constructively enhances the conditional evolution of the ^{13}C state, and thereby increases its entanglement with the NV spin.

To describe the experimental sequence shown in Fig. 1(b), we consider the mutual interaction between a single NV electronic spin-1 and a single ^{13}C nuclear spin-$\frac{1}{2}$, which is governed by the Hamiltonian ($\hbar = 1$)

$$H = \Delta S_z^2 - \mu_e B_z S_z + (\mu_n \mathbf{B} + S_z \mathbf{A}) \cdot \mathbf{I}. \quad (1)$$

Here, $\mathbf{S}$ ($\mathbf{I}$) and μ_e (μ_n) are the electronic (nuclear) spin and magnetic moment, respectively, $\mathbf{B}$ is the external magnetic field, and $\mathbf{A}$ is the hyperfine interaction. Because of the large zero field splitting $\Delta/2\pi \simeq 2.87$ GHz, we have made the secular approximation conserving S_z. The nuclear spin evolves conditionally on the NV spin state according to $H_{\mathrm{nuc}}[m_s] = \frac{\omega_{m_s}}{2} \boldsymbol{\sigma} \cdot \mathbf{n}_{m_s}$, ($\boldsymbol{\sigma}$: Pauli spin matrices). Thus the nuclear spin precesses about an effective magnetic field axis $\hat{\mathbf{n}}_{m_s} = (\mu_n \mathbf{B} + m_s \mathbf{A})/\omega_{m_s}$ with Larmor frequency $\omega_{m_s} = |\mu_n \mathbf{B} + m_s \mathbf{A}|$ when the NV spin is in state $|m_s\rangle$. We initialize the NV spin in a superposition of $|0\rangle$ and $|1\rangle$ and apply a periodic series

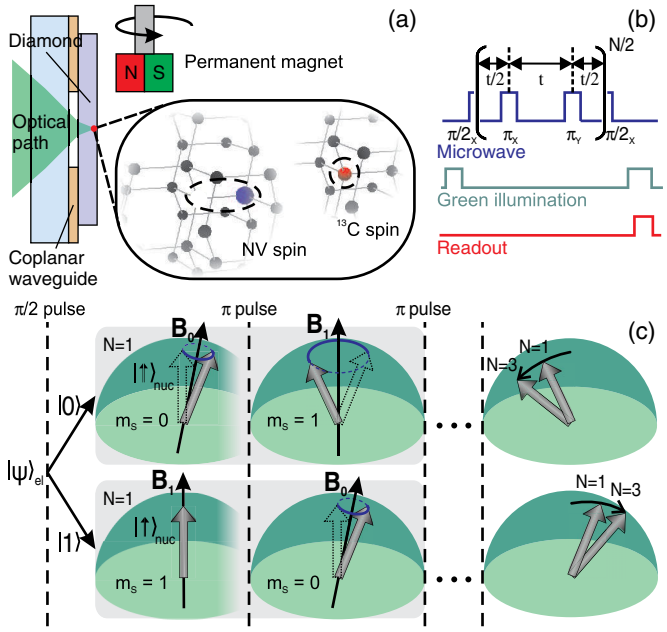

FIG. 1 (color online). (a) Schematic setup. We measure NV centers weakly coupled to ^{13}C nuclear spins. A dc magnetic field is applied using a movable permanent magnet. (b) Pulsed spin manipulation and readout. (c) Central concept. Conditional evolution of the ^{13}C on the Bloch sphere during NV spin manipulation for ^{13}C spin initially in state $|\uparrow\rangle$, where $|\uparrow\rangle, |\downarrow\rangle_{\mathrm{nuc}}$ are defined as the eigenstates of the ^{13}C spin when the NV electron spin is in the state $m_s = 1$. Upper (lower) panel shows ^{13}C evolution with the NV spin is initially in state $|0\rangle$ ($|1\rangle$). Gray boxes show evolution during spin echo (single π pulse). Additional π pulses push the conditional nuclear spin evolution further apart, increasing its entanglement with the NV. For clarity a sequence with an odd number of π pulses is shown; the result is qualitatively the same for the even numbered sequences used in this work, but is more difficult to visualize.

of $N\pi$ pulses spaced by evolution time t, during which $|0\rangle$ and $|1\rangle$ accumulate a relative phase. Converting the phase into a population difference, the normalized fluorescence signal at the end of the measurement of total length Nt is $p = (\mathcal{S} + 1)/2$, where

$$\mathcal{S} = 1 - (\hat{\mathbf{n}}_0 \times \hat{\mathbf{n}}_1)^2 \sin^2\left(\frac{\omega_0 t}{2}\right) \sin^2\left(\frac{\omega_1 t}{2}\right) \frac{\sin^2(N\phi/2)}{\cos^2(\phi/2)} \qquad (2)$$

and $\cos\phi = \cos\frac{\omega_0 t}{2} \cos\frac{\omega_1 t}{2} - \hat{\mathbf{n}}_0 \cdot \hat{\mathbf{n}}_1 \sin\frac{\omega_0 t}{2} \sin\frac{\omega_1 t}{2}$. This is the extension for arbitrary (even) N pulses of the well-known result for $N = 1$ corresponding to Hahn spin echo [5]. The factor of N multiplying the small angle ϕ is responsible for the enhanced signal that enables detection of weakly coupled nuclear spins.

Experiment.—We study NVs implanted in a diamond sample with naturally abundant spin-$\frac{1}{2}$ ^{13}C (1.1% abundance). The NV electronic orbital ground state is a spin triplet which can be initialized in the $|m_s = 0\rangle$ state using green illumination, and read out via spin-dependent

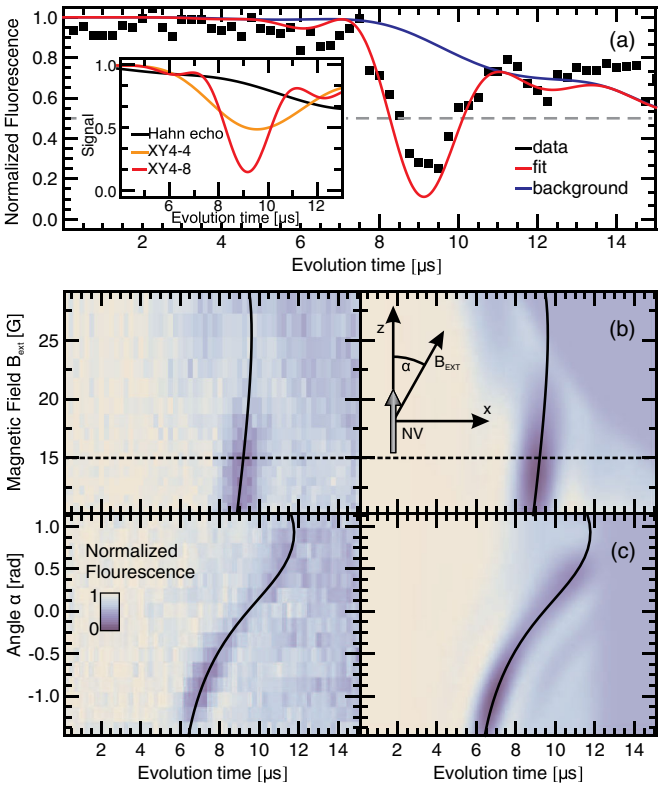

FIG. 2 (color online). Coherent interaction of an NV-Center with a single ^{13}C detected using XY4-8. (a) The evolution time between π pulses t is swept with a fixed magnetic field of 15 G, data (black) and fit (red). The blue line is the calculated response without the individual ^{13}C. The inset shows the calculated response to Hahn echo, XY4-4, and XY4-8. (b) The fluorescence is plotted as a function of t and magnetic field strength B, with magnetic field oriented along the NV $\hat{z}$ axis ($\alpha = 0$, as defined in the inset). The dashed line highlights the data shown in (a). (c) Fluorescence as a function of t and magnetic field orientation α, with $B = 19$ G. The black line displays the extracted dip position in both (b) and (c).

fluorescence [5]. The $|m_s = \pm 1\rangle$ degeneracy is lifted by a dc field applied using a permanent magnet. We coherently manipulate the NV spin using resonant microwaves delivered by a coplanar waveguide. The control pulse sequence used in this work is known as XY4-8 [14], and consists of $N = 8$ π pulses as shown in Fig. 1(b), phase alternated to mitigate microwave pulse errors.

Detection of a single weakly coupled ^{13}C spin is shown in Fig. 2(a). The dip in the NV fluorescence signal at evolution time $t \approx 9$ μs results from the coherent interaction with the single ^{13}C spin and represents the signal. Importantly, this signal would go undetected using spin echo, as shown in the inset of Fig. 2(a). That the dip drops below a normalized fluorescence of 0.5 reflects the coherent nature of the interaction. By adding microwave control over the ^{13}C, this interaction could be exploited to perform a coherent rotation of the ^{13}C spin conditional on the state of the NV electron spin or vice versa. The overall decay is a

result of the Larmor precession of the surrounding bath of distant ^{13}C spins, which produces collapses and revivals in the NV coherence [5], with only the first collapse visible in Fig. 2. The slight discrepancy between the data and the theory curve at $\sim$14 μs is a result of the random distribution of ^{13}C spins in the bath, which our model does not account for exactly [25].

To confirm that the observed feature arises from a single ^{13}C, we plot the measured signal as a function of applied magnetic field strength [Fig. 2(b)] and orientation [Fig. 2(c)]. We measure the NV response in both possible sets of magnetic sublevels ($|0\rangle \leftrightarrow |1\rangle$ and $|0\rangle \leftrightarrow |-1\rangle$, see [25]) and the entire data set is simultaneously fitted to Eq. (2). The only free parameters are the hyperfine vector $\mathbf{A}$, composed of three parameters defined relative to the NV axis and magnetic rotation axis, and two free parameters describing the strength and spectral width of the surrounding spin bath [25]. The calculated signal using the extracted fit parameters is shown in the right panels of Fig. 2, and is in good agreement with the data. We obtain a robust, unique fit over a wide range of initial parameters. The fit gives a total coupling strength of $|\mathbf{A}|/2\pi \sim 125$ kHz, which is less than the bare dephasing rate of this NV, $1/T_2^* = 400 \pm 16$ kHz. T_2^* is measured using a Ramsey sequence (shown in [25]), and arises from the bath spin configuration varying from measurement to measurement. This demonstrates that we can simultaneously decouple the NV from the ^{13}C spin bath and still obtain a measurable signal from a target nuclear spin.

Figure 3 shows the measurement of the weakest coupled individual ^{13}C observed in this work. This single spin produces no discernible signal for the evolution times and magnetic field strengths shown in Fig. 2 (measurement shown in [25]), because the weaker hyperfine coupling results in a dip that occurs after the first collapse induced by the bath and is therefore suppressed. In order to measure this weakly coupled spin at longer evolution times we increase the magnetic field, moving a bath-induced revival into the range of interest. We thereby observe a characteristic dip in the bath revival resulting from an individual nuclear spin. Again, this data is reproduced by a fit to our model; the extracted coupling strength is $|\mathbf{A}|/2\pi \sim 47$ kHz, a factor of $\sim$4.6 below the measured $1/T_2^* = 217 \pm 9$ kHz [25].

Our technique also allows us to observe the impact of multiple ^{13}C spins coupled to a single NV. As the maximum mutual interaction strength of two ^{13}C spins on adjacent lattice sites is only 2 kHz [26], we can treat the ^{13}C spins as independent. Consequently, the signal given by Eq. (2) becomes a product of the individual contributions from each coupled spin, $\mathcal{S} = \Pi_j \mathcal{S}_j$ [5]. Figure 4 shows the impact of three ^{13}C spins. The double dip visible in the data results from the product of two overlapping dips from two ^{13}C spins with similar coupling strengths. This is emphasized in the inset of Fig. 4(c), where the calculated effect of each ^{13}C spins on $\mathcal{S}$ is displayed separately. The

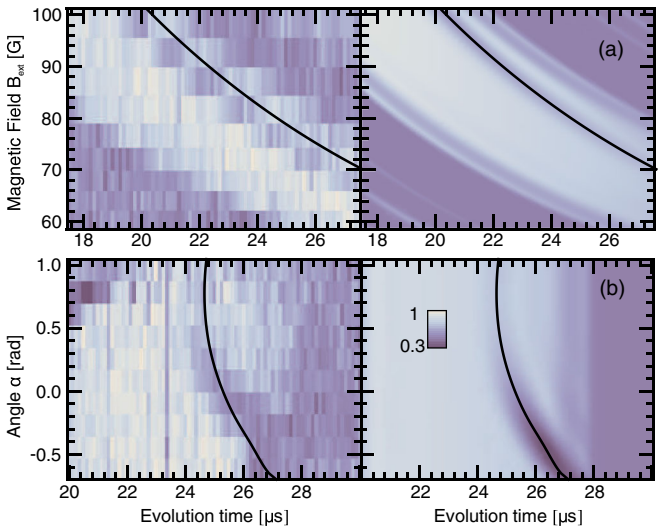

FIG. 3 (color online). Detection of a distant ^{13}C with a XY4-8 sequence. As in Fig. 2 the NV fluorescence is shown as a function of (a) magnetic field strength B with $\alpha = 0.26$ rad, and (b) magnetic field orientation α, with $B = 80$ G. The dip from the single ^{13}C is visible within a spin-bath revival centered at $2 \times 2\pi/\omega_0$.

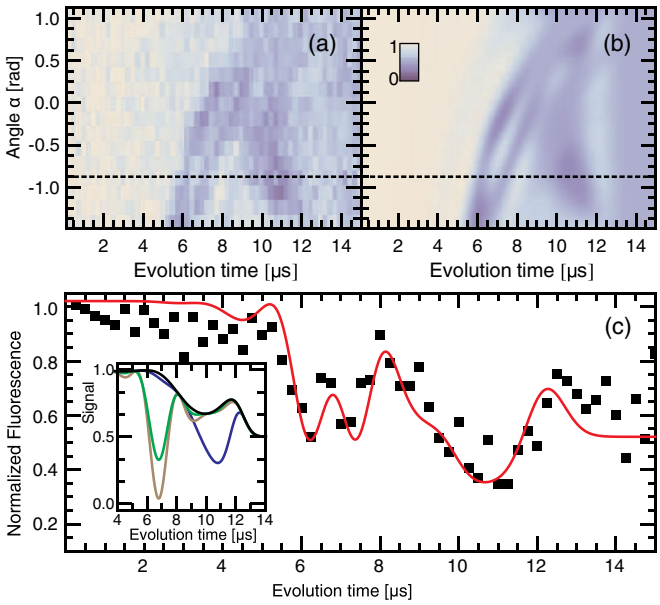

FIG. 4 (color online). Simultaneous detection of three ^{13}C nuclei. (a) and (b) NV fluorescence is shown vs evolution time t and magnetic field orientation α (data and fit), the applied field strength is 19 G. The fit assumes three ^{13}C spins and yields robust and unique individual coupling strengths, while fits assuming fewer ^{13}C spins could not reproduce the data. The NV response along the dashed line is shown in (c) black, red: data, fit. The traces in the inset display the calculated response of the NV interacting separately with each ^{13}C, and with the spin bath alone (black).

weakest coupled of the three ^{13}C spins has an extracted coupling strength of $|\mathbf{A}|/2\pi \sim 64$ kHz, a factor of ~ 8 below the measured $1/T_2^* = 560 \pm 60$ kHz [25]. By tuning the evolution time and magnetic field, the NV can be individually entangled with each of these ^{13}C spins [25]. This method could also be used to detect a larger number of individual spins, as long as their hyperfine couplings are within the detection limits imposed by the NV coherence time, as discussed in the following section.

Discussion.—Assuming the NV-^{13}C couplings arise solely from a point-dipole interaction, the measured couplings translate into NV-^{13}C distances of $\sim$0.4–0.8 nm [25], consistent with the range expected for a probabilistic distribution of naturally abundant ^{13}C. However, *ab initio* calculations suggest that the electronic wave function is non-negligible at this length scale, and may lead to a significant contact term in the hyperfine interaction [20–23]. The coupling strengths measured here significantly exceed the accuracy of state of the art calculations [20,21,23], preventing us from explicitly including the calculated contact interaction. We therefore conclude that assuming a purely dipolar interaction likely provides a minimum distance estimate. By using our technique to acquire a much larger data set in the spirit of recent surveys of strongly coupled ^{13}C spins [22,23], it should be possible to identify individual distant ^{13}C lattice sites and shed light on the spatial distribution of the electronic wave function beyond the limits of current theory.

The hyperfine couplings $|\mathbf{A}|/2\pi$ extracted in this work exceed the decoherence rate $1/T_2$ obtained in a Hahn spin echo sequence, and in principle the ^{13}C spins could therefore be detected using only a single π pulse [25]. However, this would require precise optimization of the magnetic field strength and orientation, which is not practical in a typical experiment. One advantage of extended pulse sequences is to relax these conditions and greatly simplify the identification of nuclear spins whose couplings to the NV are initially unknown. As a result, using the presented technique we were able to detect the closest ^{13}C for every NV investigated.

The use of dynamical decoupling sequences with multiple π-pulses has the added benefit of decoupling the NV spin from the surrounding environment, increasing its coherence time from T_2 to $T_2^{\text{eff}} = T_2 N^{2/3}$ and thereby potentially improving the sensitivity. Increasing the number of π-pulses for the same total evolution time requires higher magnetic fields to ensure that the sequence remains synchronized with the evolution of the target nuclear spin. In this limit $|\mu_n \mathbf{B}| \gg |\mathbf{A}|$, and a weakly coupled single ^{13}C has the same Larmor precession frequency as the surrounding nuclear spin bath and cannot be isolated. Therefore $|\mathbf{A}|/2\pi > 1/T_2$ is the limit for the detection of individual ^{13}C nuclear spins in a sample of natural isotopic abundance. However, for applications involving the detection of spins with a different gyromagnetic ratio than the surrounding bath we find the sensitivity scales with number of π pulses as $N^{4/3}$ [25]. As a result, our approach could potentially be used to detect individual spins inside or outside the diamond lattice up to the ultimate limit $|\mathbf{A}|/2\pi > 1/2T_1$, where $1/T_1$ is the NV spin relaxation rate. At room temperature $1/2T_1$ can be as low as $\sim$100 Hz [27,28], corresponding to the dipolar coupling between an NV and a proton spin at a distance of $\sim$7–9 nm, which is of great interest for single spin MRI applications [1–3].

In conclusion, we used coherently controlled single NV electronic spins to detect distant nuclear spins. In particular, extended pulse sequences enabled the detection of ^{13}C nuclei with couplings far below the electronic spin bare dephasing rate. We also demonstrated that the simultaneous detection of several distant ^{13}C spins is possible, even within an environment consisting of a large number of spins with the same gyromagnetic ratio. Our technique allows for sensitive, coherent measurements of the nuclear spin environment of a single electronic spin; moreover, extensions of this approach could be used to exploit the nuclear spin environment as a resource to extend the size of controllable multispin quantum registers. Potential novel applications range from information storage to environment-assisted sensing and single spin MRI.

We thank Jack Harris, Lillian Childress, Adam Gali, Ronald Hanson, and Tim Taminiau for stimulating discussions, and Alexander Zibrov for early contributions to the experiment. This work was supported in part by the National Science Foundation (NSF), the Center for Ultracold Atoms (CUA), ARO MURI, DARPA QUASAR, EU DIAMANT, and the Packard Foundation. S. K. acknowledges support by the DOD through the NDSEG Program, and the NSF through the NSFGRP under Grant No. DGE-1144152. Q. U. acknowledges support from Deutschen Forschungsgemeinschaft. S. K and Q. P. U. contributed equally to this work.

Note added.—Following submission of this work two complementary studies appeared [29,30] in which the technique demonstrated in this work was used to resolve individual ^{13}C nuclei weakly coupled to a single NV in the high magnetic field regime [29], and in isotopically purified diamond with depleted ^{13}C nuclei [30].

*To whom correspondence should be addressed.
quirin@physics.harvard.edu

[1] D. Rugar, R. Budakian, H. Mamin, and B. Chui, Nature (London) **430**, 329 (2004).
[2] C. L. Degen, M. Poggio, H. J. Mamin, C. T. Rettner, and D. Rugar, Proc. Natl. Acad. Sci. U.S.A. **106**, 1313 (2009).
[3] P. C. Hammel and D. V. Pelekhov, *Handbook of Magnetism and Advanced Magnetic Materials* (Wiley, New York, 2007), Vol. 5, Chap. 4.
[4] F. Jelezko, T. Gaebel, I. Popa, M. Domhan, A. Gruber, and J. Wrachtrup, Phys. Rev. Lett. **93**, 130501 (2004).

[5] L. Childress, M. V. Gurudev Dutt, J. M. Taylor, A. S. Zibrov, F. Jelezko, J. Wrachtrup, P. R. Hemmer, and M. D. Lukin, Science **314**, 281 (2006).
[6] R. Hanson, V. V. Dobrovitski, A. E. Feiguin, O. Gywat, and D. D. Awschalom, Science **320**, 352 (2008).
[7] M. V. Gurudev Dutt, L. Childress, L. Jiang, E. Togan, J. Maze, F. Jelezko, A. S. Zibrov, P. R. Hemmer, and M. D. Lukin, Science **316**, 1312 (2007).
[8] L. Jiang, J. S. Hodges, J. R. Maze, P. Maurer, J. M. Taylor, D. G. Cory, P. R. Hemmer, R. L. Walsworth, A. Yacoby, A. S. Zibrov *et al.*, Science **326**, 267 (2009).
[9] T. van der Sar, Z. H. Wang, M. S. Blok, H. Bernien, T. H. Taminiau, D. M. Toyli, D. A. Lidar, D. D. Awschalom, R. Hanson, and V. V. Dobrovitski, Nature (London) **484**, 82 (2012).
[10] P. Neumann, J. Beck, M. Steiner, F. Rempp, H. Fedder, P. R. Hemmer, J. Wrachtrup, and F. Jelezko, Science **329**, 542 (2010).
[11] L. Robledo, L. Childress, H. Bernien, B. Hensen, P. F. A. Alkemade, and R. Hanson, Nature (London) **477**, 574 (2011).
[12] P. C. Maurer, G. Kucsko, C. Latta, L. Jiang, N. Y. Yao, S. D. Bennett, F. Pastawski, D. Hunger, N. Chisholm, M. Markham *et al.*, Science **336**, 1283 (2012).
[13] J. M. Taylor, P. Cappellaro, L. Childress, L. Jiang, D. Budker, P. R. Hemmer, A. Yacoby, R. Walsworth, and M. D. Lukin, Nature Phys.**4**, 810 (2008).
[14] G. de Lange, Z. H. Wang, D. Ristè, V. V. Dobrovitski, and R. Hanson, Science **330**, 60 (2010).
[15] L. T. Hall, C. D. Hill, J. H. Cole, and L. C. L. Hollenberg, Phys. Rev. B **82**, 045208 (2010).
[16] B. Naydenov, F. Dolde, L. T. Hall, C. Shin, H. Fedder, L. C. L. Hollenberg, F. Jelezko, and J. Wrachtrup, Phys. Rev. B **83**, 081201 (2011).
[17] G. de Lange, D. Riste, V. V. Dobrovitski, and R. Hanson, Phys. Rev. Lett. **106**, 80802 (2011).
[18] C. A. Ryan, J. S. Hodges, and D. G. Cory, Phys. Rev. Lett. **105**, 1 (2010).
[19] Z.-H. Wang, G. de Lange, D. Ristè, R. Hanson, and V. V. Dobrovitski, Phys. Rev. B **85**, 155204 (2012).
[20] A. Gali, M. Fyta, and E. Kaxiras, Phys. Rev. B **77**, 1 (2008).
[21] A. Gali, Phys. Rev. B **80**, 241204 (2009).
[22] B. Smeltzer, L. Childress, and A. Gali, New J. Phys. **13**, 025021 (2011).
[23] A. Dréau, J.-R. Maze, M. Lesik, J.-F. Roch, and V. Jacques, Phys. Rev. B **85**, 134107 (2012).
[24] J. R. Maze, P. L. Stanwix, J. S. Hodges, S. Hong, J. M. Taylor, P. Cappellaro, L. Jiang, M. V. Gurudev Dutt, E. Togan, A. S. Zibrov *et al.*, Nature (London) **455**, 644 (2008).
[25] See Supplemental Material at http://link.aps.org/supplemental/10.1103/PhysRevLett.109.137601 for derivations of the equations, additional complementary data, and a table summarizing the extracted parameters for all NVs investigated in this work.
[26] N. Zhao, J.-L. Hu, S.-W. Ho, J. T. K. Wan, and R. B. Liu, Nature Nanotech. **6**, 242 (2011).
[27] A. Jarmola, V. M. Acosta, K. Jensen, S. Chemerisov, and D. Budker, arXiv:1112.5936.
[28] G. Balasubramanian, P. Neumann, D. Twitchen, M. Markham, R. Kolesov, N. Mizuochi, J. Isoya, J. Achard, J. Beck, J. Tissler *et al.*, Nature Mater. **8**, 383 (2009).
[29] T. H. Taminiau, J. J. T. Wagenaar, T. van der Sar, F. Jelezko, V. V. Dobrovitski, and R. Hanson, following article, Phys. Rev. Lett. **109**, 137602 (2012).
[30] N. Zhao, J. Honert, B. Schmid, J. Isoya, M. Markham, D. Twitchen, F. Jelezko, R.-B. Liu, H. Fedder, and J. Wrachtrup, arXiv:1204.6513.